A Numerical Analysis on Three-Dimensional Flow Field in a Supersonic Bump-Type Inlet

Sang Dug Kim
School of Automotive, Industrial and Mechanical Engineering, Daegu University, 214-1 Dea-dong, Gyeongsan-si, Gyeongsangbuk-do 712-749, Korea
Dong Joo Song*
School of Mechanical Engineering, Yeungnam University, 214-1 Dea-dong, Gyeongsan-si, Gyeongsangbuk-do 712-749, Korea

The characteristic of a supersonic inlet system with three-dimensional bump which is substituted for the diverter or conventional ramp-type compression systems has been studied numerically. A comprehensive numerical analysis has been performed to understand the three-dimensional flow field including shock/boundary layer interaction and growth of turbulent boundary layer that might occur around a three-dimensional bump in a supersonic inlet. The current numerical simulations showed the supersonic bump-type inlet which is modified from a conventional ramp-type inlet to control shock/boundary layer interaction effectively and evolved to maximize inlet performance.

Key Words : Supersonic Inlet Design, High Speed Flow, Shock/Boundary Layer Interaction, Turbulent Flow, Numerical Simulation

Nomenclature

A : Sonic speed
D : Characteristic length
D_o: Exit diameter of inlet diffuser
M : Mach number
p : Pressure
V : Speed of flow
X : Axis in streamwise direction
Y : Axis in normal direction
y_n : Normal distance from the wall surface
Z : Axis in spanwise direction

Subscripts

o : Stagnation property
t : Total property
∞ : Freestream value

* Corresponding Author,
E-mail : djsong@yumail.ac.kr
TEL : +82-53-810-2449; **FAX** : +82-53-810-4627
School of Mechanical Engineering, Yeungnam University, 214-1 Dea-dong, Gyeongsan-si, Gyeongsangbuk-do 712-749, Korea. (Manuscript **Received** July 14, 2006; **Revised** December 4, 2006)

1. Introduction

A supersonic inlet has to provide homogeneous, low speed and high pressure air flow to the compressor face of an engine with over a wide range of speeds, altitudes, and maneuvering conditions. It must be designed to produce the lowest drag, weight, cost, and the highest propulsion performance. The complexity of inlet system becomes serious as the top speed of aircraft increases. These devices are assembled to compress air flow from supersonic to subsonic level before it reaches the face of the engine. These compression devices play an important role in the conversion of the kinetic energy of high speed flow into static pressure before the compressor face of the engine. Higher speed aircrafts generally require more complicated compression systems such as a series of movable compression ramps, porous walls, slots controlled by sophisticated software and complex mechanical systems (Gridley and Walker, 1996). In a high-speed supersonic aircraft configuration

(e.g., $M_\infty=2\sim5$), a compression system produces an oblique shock wave externally to reduce flow speed from freestream value, followed by normal shock wave near the inlet through which flow becomes subsonic. The interaction of a shock wave with a turbulent boundary layer yields large adverse pressure gradients causing rapid thickening and possible separation of the boundary layer. The resulting shock/boundary layer interactions may lead to total pressure losses and distorted boundary layer profiles that can seriously degrade engine performance. Therefore, inlet designs of high speed aircraft must consider the removal of the boundary layer which contains low-energy air that flows along the surface of the fuselage and inlet at subsonic and supersonic speeds. The boundary layer thickens with increased fore-body distance, the length from the nose of an aircraft to the inlet itself. A supersonic aircraft was dealt with this boundary layer phenomenon by redirecting airflow such as a diverter of a gap between the fuselage and the upper lip of the inlet or the combinations of splitter plates and bleed systems (Seddon and Goldsmith, 1999). The bleeding flow which may remove the thick boundary layer inside the diffuser can consume a significant fraction of the ingested inlet mass flow, and the amount required increases as Mach number increases (Nicolai, 1975 ; Benson and Miller, 1991 ; Anderson, 1990). The bleeding mass flow reaches up to 15% of engine mass flow at Mach 2 which is proportional to the drag penalty. An aircraft eliminating the bleeding system, however, can reduce the empty weight reduction up to 12% (Loth, 2000).

The concept of three-dimensional surface to control the boundary layer in supersonic inlet flow has been investigated. Simon et al. studied an external bump-type inlet with boundary-layer bleeding, which yielded satisfactory operational stability over a range of Mach numbers from 1.5 to 2 (Simon et al., 1957). A three-dimensional bump (Fig. 1) installed in the supersonic inlet may play a role as a compression surface and a removal system of upstream boundary layers that prevents the low-energy airflow from entering the inlet instead of complex and heavy mechanical bleeding systems (Seddon and Goldsmith, 1999 ; Tillotson et al., 2006). Therefore, it is of interest to study the effectiveness of compression systems using a bump on shock/boundary-layer interactions in high-speed inlet flow.

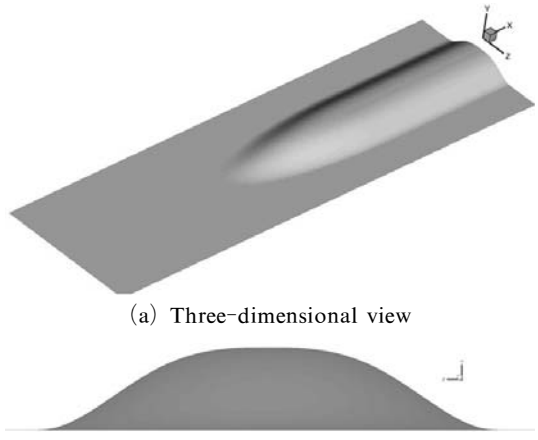

(a) Three-dimensional view

(b) Front view

Fig. 1 Geometry of a three-dimensional bump

2. Numerical Method

2.1 Governing equation

The present three-dimensional computational analysis of supersonic inlet flows generating an oblique shock wave was carried out using the numerical method (Kim and Song, 2005a) that integrates the governing equations on structured grids with a second-order upwind implicit scheme (Hirsh, 1989) for the convection terms of the conservation equations. The flow was modeled with the Reynolds-averaged Navier-Stokes equations for a thermally and calorically perfect gas, employing the Boussinesq hypothesis for turbulence modeling. The shear stress transport (SST) turbulence model was selected to close the Reynolds-averaged conservation equations because of its superior performance and stability as compared to other turbulence models for adverse pressure flows as shown in previous investigations (Kim and Song, 2005b ; Kim et al., 2004). The details of the conservation equations and the turbulence model are well documented in the above literature. Figure 2 shows the applications for the supersonic compression corner cases, which imply the strong shock/boundary-layer interaction. The

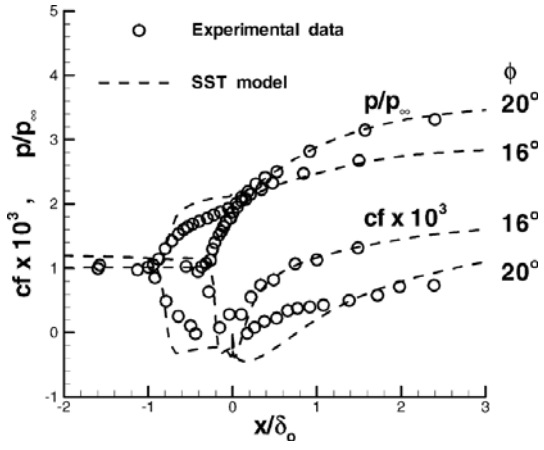

Fig. 2 Wall pressure and skin friction coefficient distributions showing comparison of the current numerical simulation with the experimental data of Settles et al.(1979) for 16- and 20-deg ramps

freestream Mach number was 2.85, and two different ramp angles were 16 and 20 deg. The experiments of Settles et al.(1979) deal with the ramp placed on the bottom wall of a wind tunnel to allow the shock to occur, which interferes with turbulent boundary layer. The SST turbulence model used in this work produces a good rate of skin-friction coefficient recovery and wall pressure distribution downstream of the shock.

2.2 Grid system and boundary conditions

In this work on the flow characteristics around the bump in supersonic flow, a simple bump installed on the flat plate under the top cover (cowl) has the maximum height of $Y/D \approx 2$. The inlet and outlet exits in the computational domain were far ($X/D \approx \pm 20$) in streamwise direction from the bump top ($X/D=0.0$) where is the highest location of the three-dimensional shape of the bump.

In order to obtain solutions to the conservation equations, proper boundary conditions are needed for the computational domain. At the inflow boundary of the inlet, the incoming flow properties were prescribed by the profiles obtained from the solution of a flat plate turbulent boundary layer flow. At the outflow boundary where airflow exited the computational domain without normal shock wave in the interior of the inlet, the flow is mostly supersonic except for a small region near the wall, so that all flow variables were extrapolated. The back pressure was, however, specified for the outflow boundary condition in order to generate normal shock waves within internal inlet flow field. The no-slip boundary condition and adiabatic wall condition were imposed on the wall surfaces. The grid system is composed of 6 blocks in which each one has over the $4 \times 10^{+5}$ mesh points. The viscous mesh placed a first grid point from the wall at y^+ less than unity. A stretching function was used to cluster grid points near the wall and shock location. Convergence of the solutions was considered to be achieved when the L^2 norm of the maximum residual reached 10^{-4}.

3. Result and Discussion

3.1 The flow characteristics near the wall surface of a bump in a supersonic flow

Three-dimensional bump installed on the flat plate in supersonic flow field makes strong three-dimensional oblique shock waves around its leading edge and induces continuous increase of static pressure along the inclined surface of the bump. When a shock wave occurs without a cowl as shown in Fig. 1, the pressure may decrease after the top of the bump ($X/D=0.0$) due to the flow expansion. These oblique shock waves may induce the increase of pressure downstream of the top of the bump due to the following reflected shock wave when it has a cowl or the normal shock wave which leads the internal flow of the inlet to be subsonic. This oblique shock wave may form a three-dimensional shape resembling the bump geometry, and airflow follows the curved surface of the bump in z-direction, which fluid comes from the symmetric plane of the bump ($Z/D=0$) toward outside region of the wall surface of the bump as shown in Fig. 3, in which these flow behavior occurs particularly near the wall surface of the bump where the flow energy is low and the flow speed is slow. Since the effect of the bump geometry eliminates low speed fluid from the thick boundary layer induced by the

shock wave, it can reduce the thickness of boundary layer on the inclined wall surface of the bump and may keep sound boundary layer for adverse pressure gradient flow in the diffuser of a supersonic inlet.

Figure 4 shows the contours of flow speed normalized by freestream sonic speed (A_∞) on the cross sections at four locations in streamwise direction of supersonic inlet flow. The thickness of boundary layer developed upstream of the bump (Fig. 4(a)) decreases rapidly (Fig. 4(b)), and becomes the thinnest on the top of bump (Fig. 4(c)). Even though the boundary layer is interfered by the reflected shock wave which faced to the bump wall surface after the reflection on the cowl, it maintains steadiness on the bump as much as the one at the inlet boundary (Fig. 4(d)). The low-velocity fluids removed from the curved surface of the bump induced the secondary flow near the corner of the side and bottom walls and increased the thickness of boundary layer. The proper design of the shape of the bump and the cowl location can resolve this problem which produces these secondary flows.

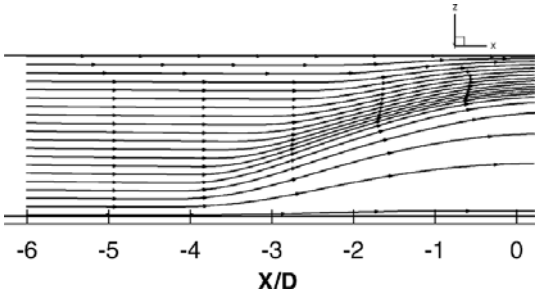

Fig. 3 Streamline around the leading edge of a three-dimensional bump

Figure 5 show the total pressure contours on four cross sections which is perpendicular to the streamwise direction of x-direction. The area where the flow has low total pressure due to viscous loss within the boundary layer at $X/D=-3$ reduced as compared with at $X/D=-6$. The area of low total pressure downstream of the bump top was minimized since the geometry of

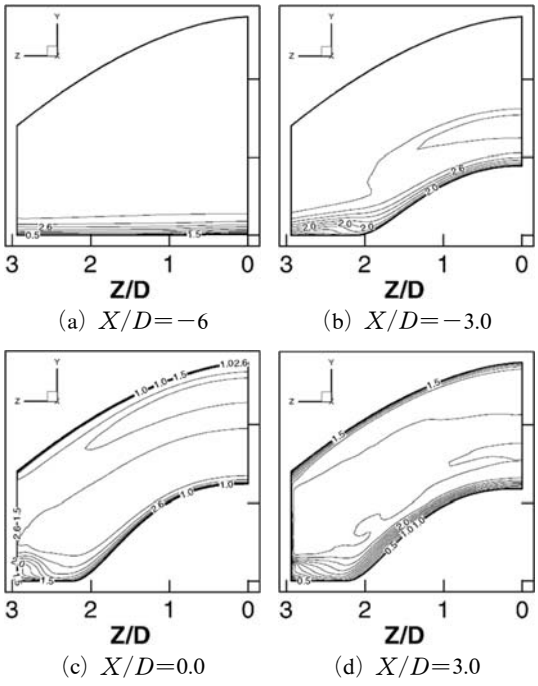

Fig. 4 Non-dimensional speed (V/A_∞) contours on the cross sections at four locations in streamwise direction for supersonic bump flow with a cowl

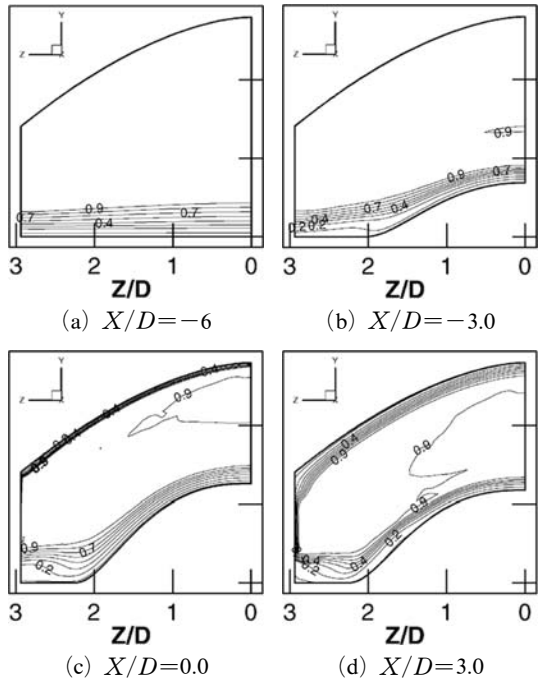

Fig. 5 Non-dimensional total pressure contours on the cross sections at four locations in streamwise direction for supersonic bump flow with a cowl

the bump pushes the low-speed flow out of the surface of the bump. So, the internal flow retains the healthy profile of the boundary layer over the wall surface of the bump ($X/D=3$ and $Z/D<2$).

The total pressure distribution and development of boundary layer in supersonic inlet flow field are important to assess the performance of supersonic inlet because their loss and non-homogeneous distribution in internal flow of inlet degrades the engine performance and may severely reduce the its lifetime of an aircraft. So, the proper design of a supersonic inlet and the flow control are critical to reduce the total pressure loss and the thickness of the wall boundary layer. In this point of view, as shown above, a three-dimensional bump has potential advantages to control the internal flow for high-quality airflow in a supersonic inlet.

Two-dimensional bump was assumed to be same domain as the symmetric plane of z-direction in three-dimensional bump flow in order to compare its flow field with three-dimensional bump flow field and to understand the effect of three-dimensional shape of a bump. As known, two-dimensional flow may generate steeper angle and stronger oblique shock wave than three-dimensional flow, and it may induce continuous development of boundary layer on the inclined surface of a two-dimensional bump, which may yield the strong shock/boundary-layer interaction following reversed flow and the sudden increase of the boundary-layer thickness after impingement of the reflected shock wave. As shown in Fig. 6 which yields the comparison of the non-dimensional speed of two- and three-dimensional bump flow, after the oblique shock wave at the leading edge of the bump in three-dimensional flow, the magnitude of the velocity profiles was reduced ($X/D=-3$, $Z/D=0$) as compared with the one at inlet boundary. But the flow near the inclined surface of the bump is redeveloped rapidly and reached a higher speed than the one at inlet boundary within the boundary layer ($X/D=0$, $Z/D=0$). It also shows a sound boundary layer profile after the interaction of reflected shock wave and boundary layer ($X/D=3$, $Z/D=0$). In the two-dimensional bump flow, however, the shock wave produced the severe distortion of velocity profile and the sudden development of the boundary layer, which yields serious non-homogeneous distribution of velocity profile downstream of the shock wave in supersonic flow field.

Figure 7 shows the comparison of total pressure profiles between two-dimensional and three-dimensional bump flow. The recovery of total

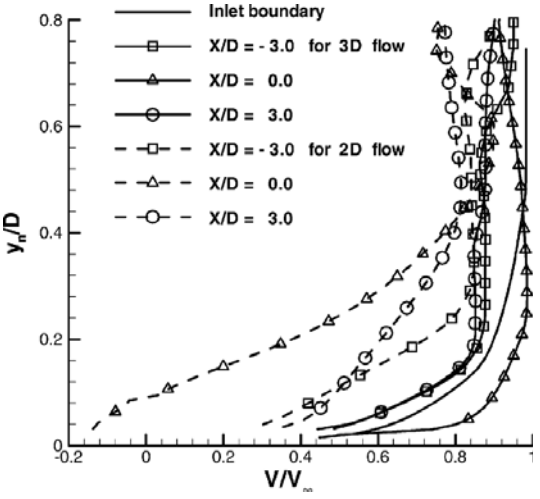

Fig. 6 Comparison of velocity profiles between two and three-dimensional bump flows

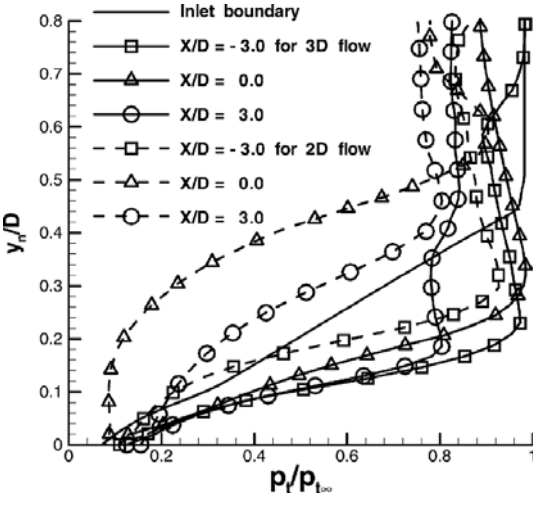

Fig. 7 Comparison of non-dimensional total pressure profiles between two and three-dimensional bump flows

pressure profile was shown within the boundary layer on the inclined surface of two-dimensional bump at $X/D=-3$. Its magnitude was, however, severely reduced near the wall surface of the bump after the interaction of reflected shock wave and boundary layer at $X/D=3$. In three-dimensional bump flow, even though the shock loss was clearly shown over $y_n/D=0.4$, the defect of total pressure near the wall surface due to viscous loss considerably reduced comparing with the one in two-dimensional flow. The effect of three-dimensional bump is clearly shown as compared with two-dimensional bump flow.

3.2 The flow characteristics in a supersonic bump-type inlet

In this investigation for a new inlet with a three-dimensional bump, the conventional ramp-type inlet was developed. The original ramp-type inlet model was tested in the experiment of Loth et al. in 2004 (Loth et al., 2004) which was conducted in the NASA Langly (LaRC) UPWT (Unitary Plan Wind Tunnel). The ramp-type inlet design was loosely based on an F-15 inlet (Fig. 8 (a)), which has a low-expansion subsonic diffuser so that any separation is related to the shock/boundary-layer interaction. The cross-sectional area was expanded in streamwise direction to lower Mach number to about 0.45 at the Aerodynamic Interface Plane (AIP), which was relied on the one-dimensional analysis of shock relationship and inviscid flow.

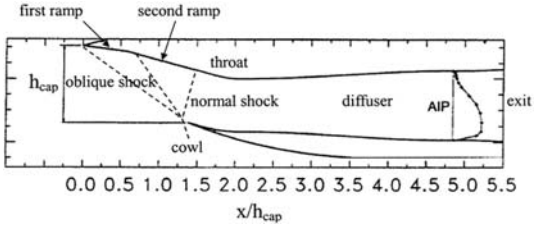

(a) Schematic diagram of a conventional ramp-type inlet based on the experiment of Loth et al. (2004)

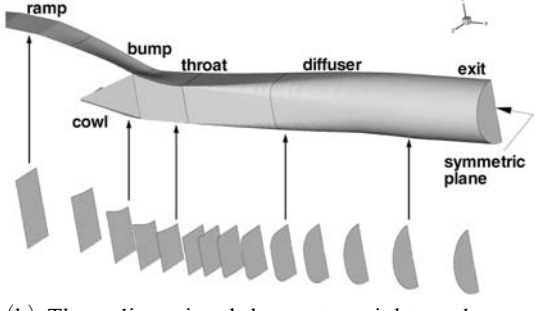

(b) Three-dimensional bump-type inlet and cross sections in streamwise direction

Fig. 8 The geometry of a supersonic ramp- type and bump-type inlet

Figure 8(b), however, shows the half geometry of a supersonic bump inlet in which flow field was assumed to be symmetric. This three-dimensional bump inlet consists of ramp, bump, throat, diffuser and cowl which were based on a conventional ramp-type inlet of Loth et al. in 2004 (Loth et al., 2004) and evolved to remove shock/boundary layer interaction effectively based on the previous study on the bump. As shown in Fig. 8(b), the parts of ramps in the original ramp-type inlet were replaced by the ramp and the bump in a bump-type inlet. In the computation domain, the inlet boundary was freestream at Mach number of 2.0, and the static pressure of the outlet boundary was specified to stand the normal shock just in front of the lip of the cowl. The grid blocks were attached on the side and the bottom of the cowl to let the low energy fluid flow and expand out of the inlet.

Figure 9 shows the non-dimensional static pressure (p/p_∞) and Mach number contours near the throat which includes two oblique and a normal shocks on the symmetric plane. It shows the severe distortion of velocity profile after the normal shock near the wall of three-dimensional bump (on upper surface), which is the shock/boundary layer interaction, but just downstream of the interaction, weak flow field was rapidly recovered to become healthy before the throat of the inlet and retain sound boundary layer in the diffuser.

It is not likely to be in a conventional ramp-type inlet in which the strong shock/boundary layer interaction induces slow flow recovery near the throat and very thick boundary layer in its downstream in Fig. 10 which is resulted from ramp-type inlet flow simulations. To remove this thick boundary the bleed system consumes a significant fraction of inlet mass flow. The amount

of bleeding flow has to increase as much as Mach number increase, and resulting penalties such as inlet drag are proportional to this bleed percentage. So, the bump-type inlet can eliminate the bleeding and the additional ducting systems, which can allow significant reduction of the empty weight for high speed vehicles (Loth et al., 2004).

Figure 11 shows the comparison of Mach number and total pressure contours on the exit plane of the supersonic bump inlet between the conventional ramp-type and three-dimensional bump-type inlets. In particular, the shock/boundary-layer interaction can produce significant total pressure losses, boundary layer thickening, separation, flow non-uniformities, and flow oscillations so that its affect results in the total pressure dis-

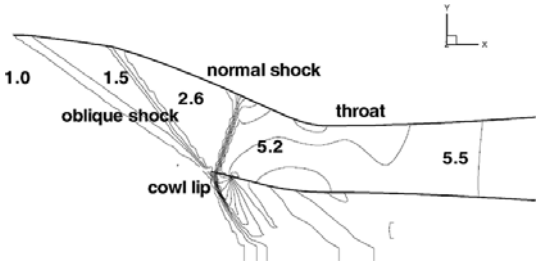

(a) Non-dimensional static pressure contours

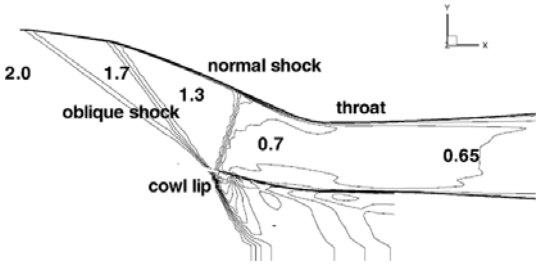

(b) Mach number contours

Fig. 9 Flow field near the throat on the symmetric plane of a supersonic bump-type inlet

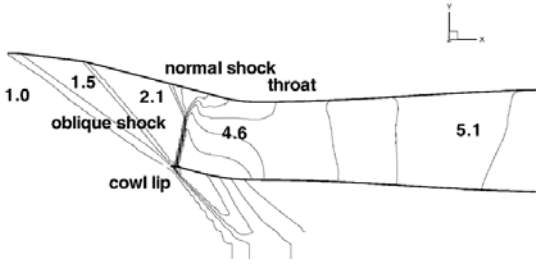

(a) Non-dimensional static pressure contours

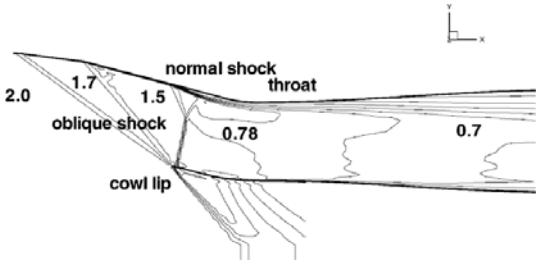

(b) Mach number contours

Fig. 10 Flow field near the throat on the symmetric plane of a conventional ramp-type inlet

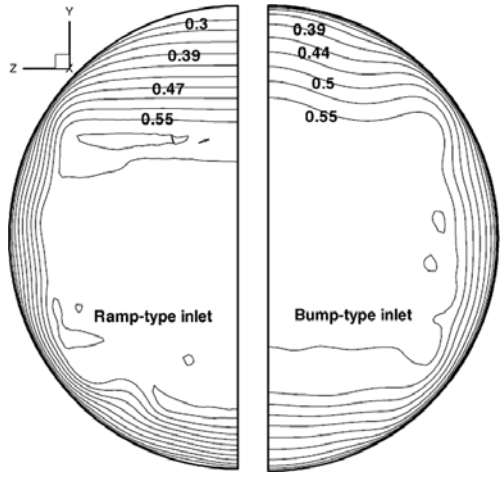

(a) Mach number

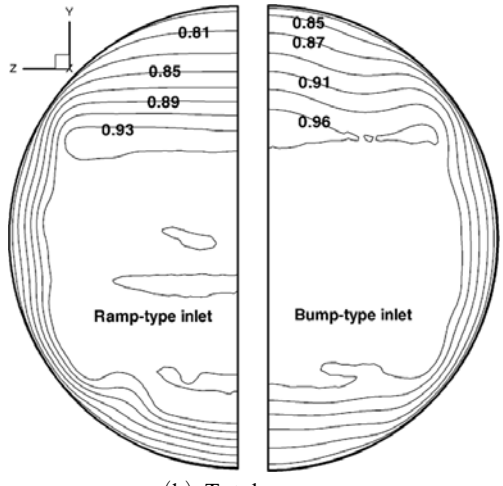

(b) Total pressure

Fig. 11 Mach number and Non-dimensional total pressure contours at the AIP showing comparison between a conventional ramp-type inlet and a bump-type inlet

tribution at the AIP. Since the low energy fluid within the boundary layer was removed effectively by the three-dimensional bump, the sound shape of boundary layer profile at the throat might produce the high total pressure recovery and uniform flow at the AIP. The bump-type inlet produced wider uniform area of total pressure and Mach number distribution as compared with the conventional ramp-type inlet. Sine all these effects can be detrimental to a propulsion system's performance and operability, the bump-type inlet has sound features and good comparison with the conventional ramp-type inlet.

Figure 12 shows the comparison of non-dimensional total pressure profiles between the conventional ramp-type and the current three-dimensional bump-type inlets which was developed from this ramp-type inlet. The total pressure profile in ramp-type inlet flow was severe distorted since the boundary layer was not recovered well after the strong shock/boundary-layer interaction and thickened under the adverse pressure gradient of the inlet diffuser. The one on symmetric plane in the bump-type inlet flow was, however, redeveloped rapidly, which can reach the high total pressure recovery and retain uniform in its profile at the AIP of a supersonic bump-type inlet as compared with the ramp-type inlet.

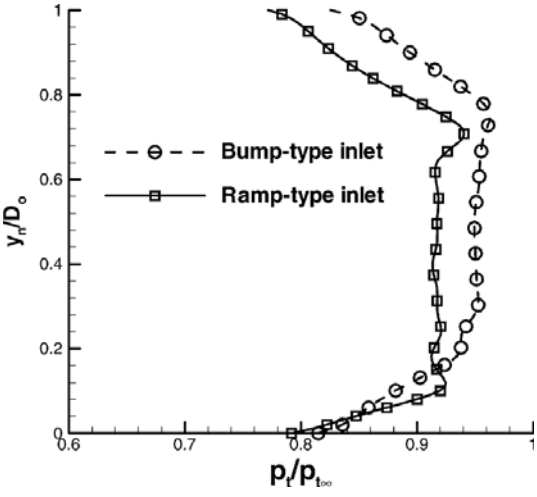

Fig. 12 Comparison of non-dimensional total pressure profiles between a conventional ramp-type inlet and a bump-type inlet at the AIP

4. Conclusions

Current study simulated supersonic inlet flow with shock/boundary layer interactions induced by a three-dimensional bump which is installed to substitute the conventional compression system in a supersonic inlet. In this study, a comprehensive numerical analysis has been performed to understand the characteristics of the shock/boundary layer interaction and growth of turbulent boundary layer that occurs around a three-dimensional bump in a supersonic inlet. The bump of a supersonic inlet plays a critical role to reduce the total pressure loss and the thickness of the wall boundary layer downstream of the shock/boundary layer interaction. The characteristics of boundary layer seen in the present numerical simulations indicate the potential capability of a three-dimensional bump to control internal flow in supersonic inlets, and the bump-type inlet may has sound features for inlet performance as compared with the conventional ramp-type inlet.

Acknowledgments

This work was partially supported by 2006 Yeungnam University 2nd stage BK21 project and a Grant No. R08-2004-000-10556-0 from Korea Science and Engineering.

References

Anderson, J., 1990, "Airframe/Propulsion Integration of Supersonic Vehicles," 26th AIAA/SAE/ASME/ASEE Joint Proportion Conference, AIAA 90-2151, Orlando, Fl, July.

Benson, J. and Miller, L. D., 1991, "Mach 5 Turbo-Ramjet Inlet Design and Performance," ISABE 91-7079, ISABE Conference, Nottingham, U.K., September, Vol. 12, pp. 746～753.

Gridley, M. C. and Walker, S. H. 1996, *Advanced Aero-Engine Concepts and Controls*, AGARD Conf. Proc. 572, 86th Symposium, Seattle, WA.

Hirsh, C., 1989, *Numerical Computation of Internal and External Flows*, Vol. 2 JOHN WILEY & SONS, NY, pp. 493～594.

Kim, S. D., Kwon, C. O. and Song, D. J., 2004, "Comparison of Turbulence Models in Shock-Wave/Boundary-Layer Interaction," *KSME International Journal*, Vol. 18, No. 1, pp. 153～166.

Kim, S. D., and Song, D. J., 2005a, "The Numerical Study on the Supersonic Inlet Flow Field with a Bump," *Journal of Computational Fluids Engineering*, Vol. 10, No. 3, pp. 19～26.

Kim, S. D. and Song, D. J., 2005b, "Modified Shear-Stress Transport Turbulence Model for Supersonic Flows," *Journal of Aircraft*, Vol. 42, No. 5, pp. 1118～1125.

Loth, E., 2000, "Smart Mesoflaps for Control of Shock Boundary-Layer Interactions," *AIAA Fluid Dynamics*, AIAA 2000-2476, Denver, CO, June.

Loth, E., Jaiman, R., Dutton, C., White, S., Roos, F., Mace, J. and Davis, D., 2004, "Mesoflap and Bleed Flow Control for a Mach 2 Inlet," 42nd AIAA Aerospace Science Meeting, AIAA 2004-855, Reno, NV, January 5～8.

Nicolai, L. M., 1975, *Fundamental of Aircraft Design*, METS Inc. San Jose, CA.

Seddon, J. and Goldsmith E.L., 1999, *Intake Aerodynamics*, pp. 336～340.

Simon, P. C., Brown, D. W. and Huff, R. G., 1957, "Performance of External-Compression Bump Inlet at Mach Number of 1.5 to 2.0," NACA-RM-E56L19, National Advisory Committee for Aeronautics, Washington.

Tillotson, B. J., Loth E. and Dutton, J. C., 2006, "Experimental Study of a Mach 3 Bump Compression Flowfield," 44th AIAA Aerospace Science Meeting and Exhibit, January 9～12, Reno, NV.